2. SOFT-SWITCHING MULTILEVEL INVERTER WITH FLYING CAPACITORS FOR ACTIVE POWER FILTER APPLICATIONS

2.1 INTRODUCTION

With significant development of power converter technologies, there has been a rise of interest in an active power filter (AF). It is now well known that an active filter can easily compensate for harmonic current contents in the load current by inserting negative harmonics into the power network [B3]-[B10].

Basic principle of an active harmonic compensation is shown in Fig. 2.1. The AF can cancel the load current harmonics generated by the static power converter, so that the ac source current is pure sinusoidal and is in phase with the input voltage. However, when the network voltage increases to a level between 2 kV and 4 kV, it is necessary to employ multilevel structures of the main circuit, even if they need double number of switches. The benefit of using a multilevel structure that uses a fraction of the high dc voltage is that it overcomes the limiting voltage and current ratings of the main switch device. Furthermore, since an AF is a type of boost converter, the high voltage is critical point at the design of the main circuit.

Fig. 2.2 shows the sample current waveforms of a three-phase active filter. This indicates that the magnitude of current in the active filter depends highly on the distortion factor and power factor of the load current. The compensating current can be calculated by various approaches. Furthermore, since the active filter supplies only reactive power, all power of the inverter should be reactive so that the inverter only circulates the current in and out. With regard to reactive

power for a three-phase system, the inverter can be implemented with small power capability because the average power of the inverter is zero as shown in Fig. 2.3. Thus, to make the inverter's average power zero, the average source power needs to be larger than the load power. However, in a practical system, the voltage controller can compensate the portion of the power losses of main switches and capacitors in the active filter [B8]-[B9].

In this chapter, a newly developed soft-switching inverter is proposed and discussed with its active power filter application. The proposed soft-switching circuit uses a zero-voltage-transition (ZVT) cell with inductor coupling, in which the auxiliary devices have less voltage and current ratings. The inverter is verified through computer simulation and experiment with a prototype inverter.

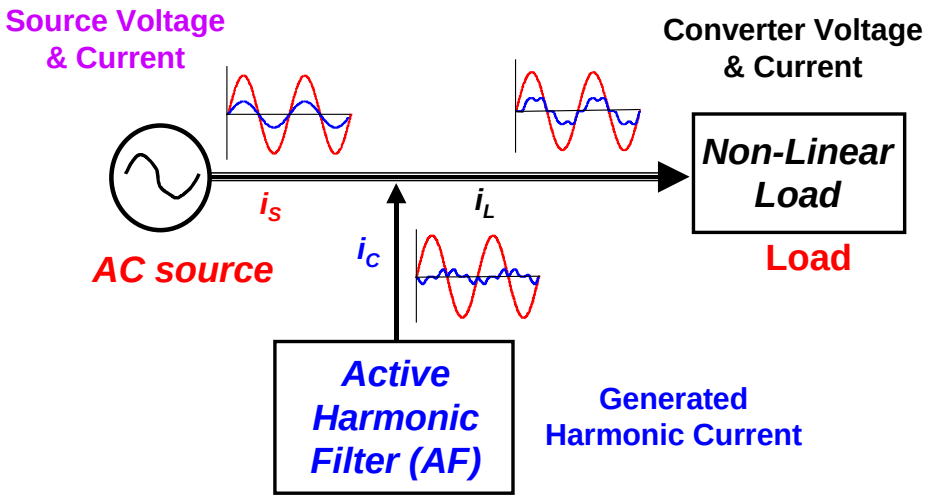

Fig. 2.1. Basic block diagram of active harmonic compensation.

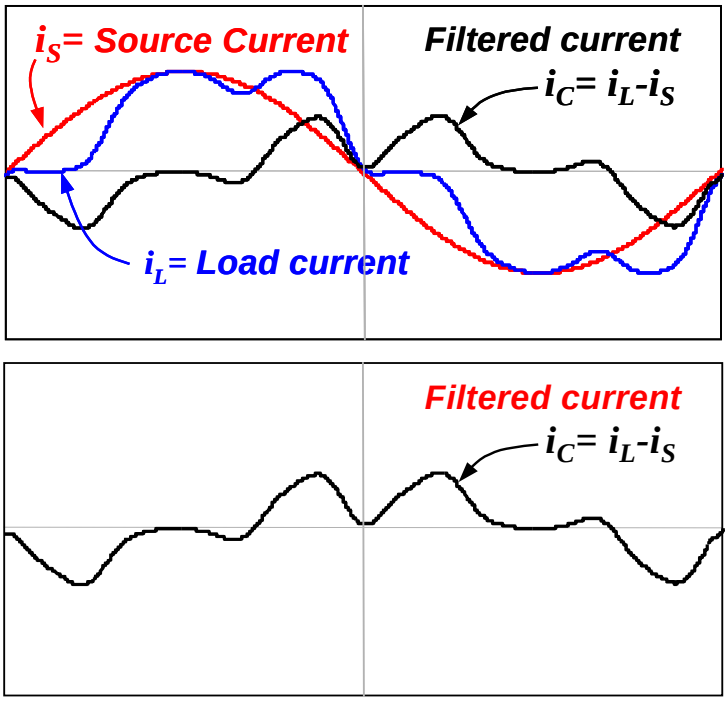

Fig.2.2. Sample current waveforms of a three-phase active power filter.

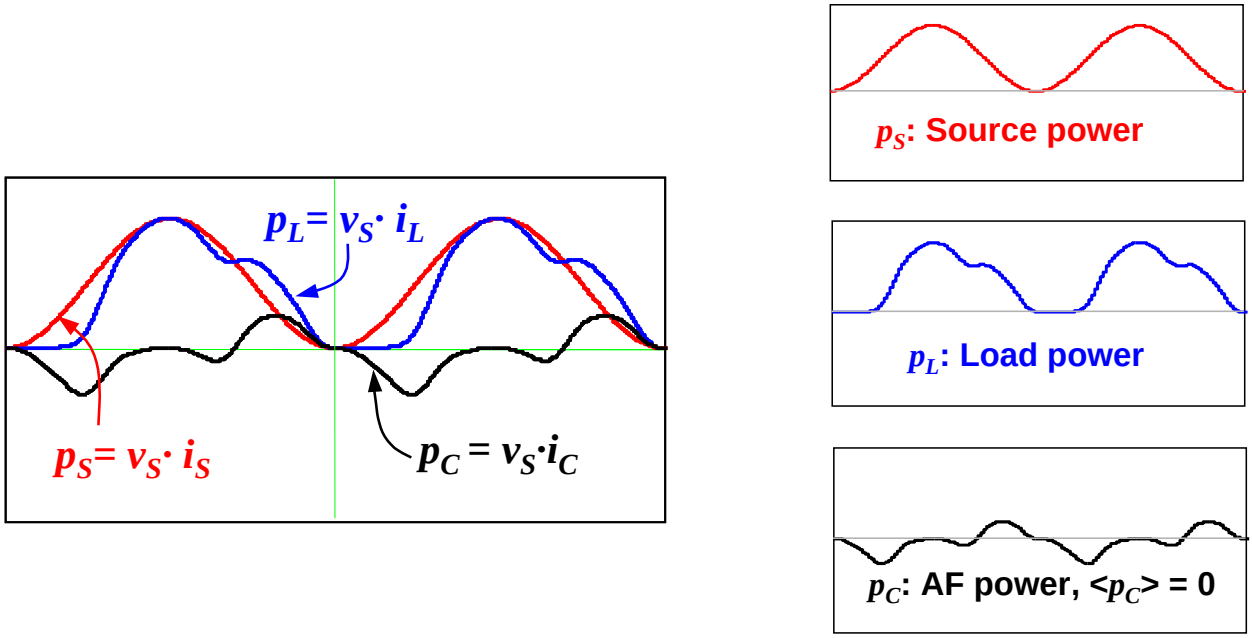

Fig. 2.3. Reactive power compensation of a three-phase system.

2.2 REVIEW OF SOFT-SWITCHING MULTILEVEL INVERTERS

Recently, soft-switching techniques are being used to reduce the switching losses and to get higher efficiency from the hard-switching inverters [D26]-[D33]. Most of researches in this area have been concentrated in the soft-switching techniques of the diode clamped multilevel inverter (DCMI) suitable for active power applications [D26], [D27], [D29] and [D32]. The DCMI can extend the power capacity with series of connected switch modules. In spite of the ease of its modularized structure, its application has been limited because of the two extra blocking diodes per leg. While clamping the turn-off voltage, a high voltage generally causes stress on these diodes. Furthermore, an additional midpoint connection makes more difficulty the practical implementation of its power packaging.

A second type of inverter structure is the flying capacitor multilevel inverter (FCMI) [D11]. It requires a flying capacitor across a two switch pair as a standard 2-level inverter at floating. By eliminating two extra clamping diodes and a neutral midpoint, in a simpler inverter structure compared to DCMI's is produced. On the other hand, the FCMI can easily overcome the static and dynamic voltage balance between the device off state voltages in the main switch, without an extra control loop to keep voltage balance between upper- and bottom-capacitors.

Until now, there has been very little work done in soft switching techniques of the flying capacitor based multilevel inverter (FCMI) [D27], [D28], and [D30]. Because the pair of switches of FCMI is connected to each floating capacitor, the soft-switching circuit generally requires high voltage rating devices. Thus, use of soft-switching techniques degrades their potential and creates design difficulties.

This study presents a new soft-switching topology suitable for FCMI applications. The topology basically consists of an inductor coupled soft-switching circuit that provides the resonant current for all of the main switches. In order to achieve zero-voltage-switching (ZVS) operations, the soft-switching cell with a coupled inductor is connected to the midpoint of the dc capacitors such as the auxiliary resonant commutate pole (ARCP) concept. Thus, the soft-

switching cell can reduce the voltage and current rating of the auxiliary switch and diode on each leg. Consequently, the proposed topology is a more attractive and desirable feature for most commercially available modules in the industry. However, a major hurdle is the bulky coupled inductor. In general, the coupled-inductor-based-inverters have large circulating and magnetizing currents through the coupled inductor. The problem associated with the coupled inductors can be solved by optimizing the design of the coupled inductor and by adding the saturable inductor to the soft-switching circuit, [D31] and [D33]. The detailed descriptions are discussed in the following subsection.

2.3 PROPOSED SOFT-SWITCHING INVERTER TOPOLOGY

Fig. 2.4 shows a single-phase three-level inverter circuit with flying capacitors. The flying capacitors are connected to each leg across the two inner loop switches, S_{2p} & S_{3p}, and S_{2n} & S_{3n}, respectively. Since these capacitor voltages can be self-balanced without the inherent feedback circuit, the stability of the flying capacitor in the FCMI can be achieved easily. Furthermore, the voltage clamping by use of the flying capacitor can be conducted directly to all the main switches in the leg. Thus, these features of the FCMI overcome benefits of the DCMIs in the motor drive and utility applications.

Fig. 2.5 shows the proposed soft-switching three-level inverter circuit with coupled inductors that can be extended to multilevel inverter applications. The soft-switching circuit includes two pairs of auxiliary switches (S_{x1}-S_{x4}), two pairs of blocking diodes (D_{x1}-D_{x4}), and two coupled inductors per phase leg. Snubber capacitors are connected to the main devices. These capacitors assist the commutation process of the main switching devices that consist of two loops, the inner and outer loop. The inner loop switches, S_2 and S_3, are alternatively switched on and off by the switching states during the first switching period, whereas the outer loop switches, S_1 and S_4, are conducting or blocking depending on the desired switching duties.

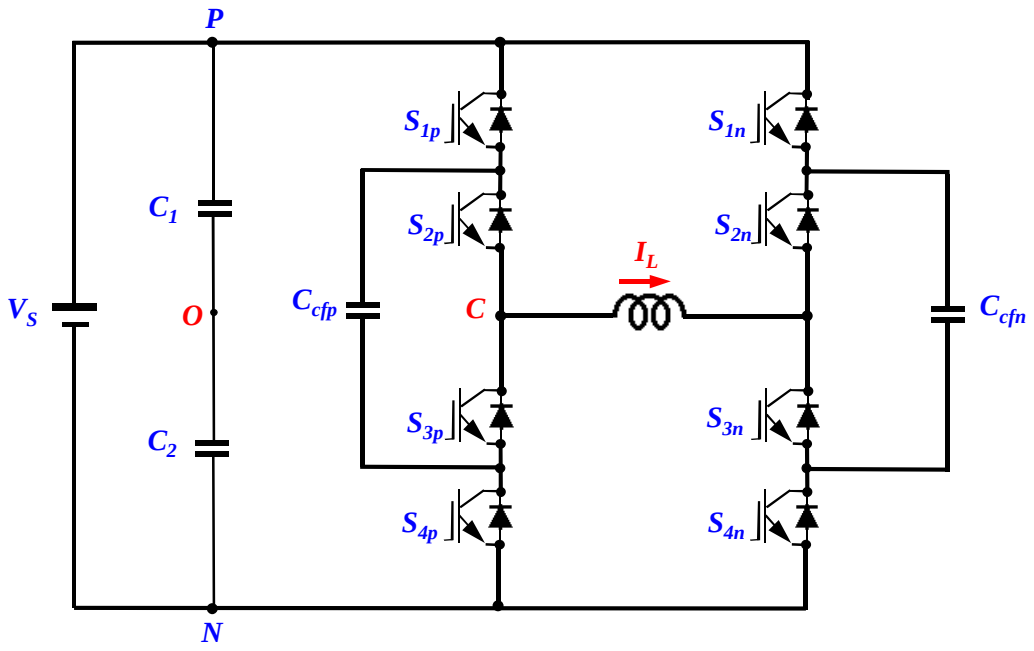

Fig. 2.4. Configuration of a single-phase three-level inverter circuit with flying capacitors.

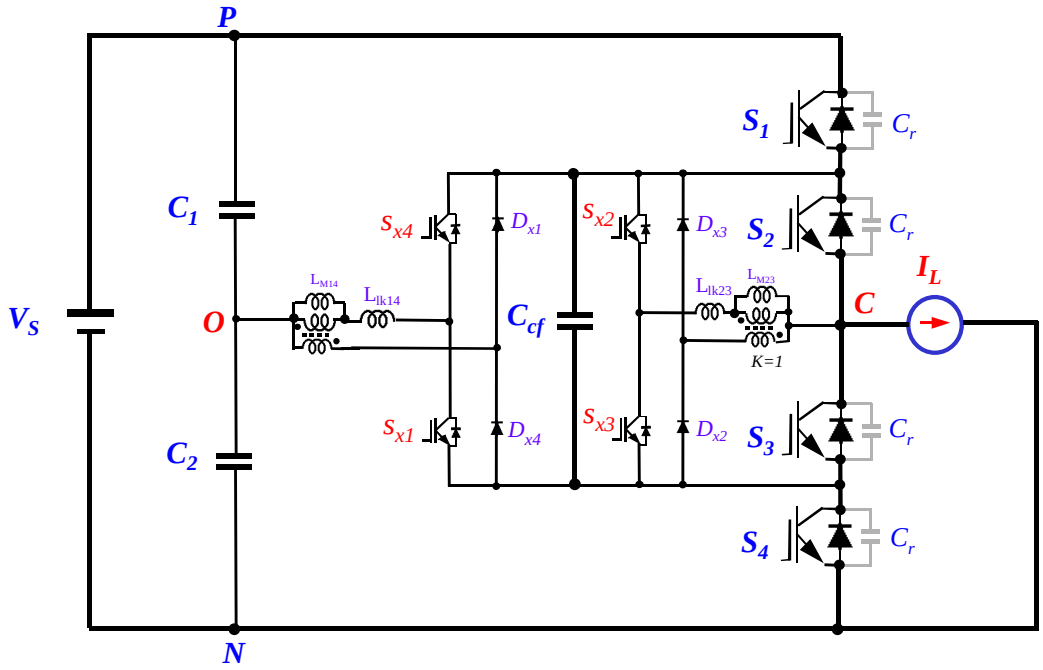

Fig. 2.5. Proposed soft-switching three-level inverter with one phase leg.

Fig. 2.6 shows the switching sequences of the FCMI. For example, under duty cycle d<0.5, the inverter has three different operational modes to achieve the desired output voltage waveforms when the load current is positive. In order to get the voltage balancing of the flying capacitors, symmetrical switching modulation is required. The switching sequence presents the following order with a cyclic sequence such as I-II-III-II-I. According to the switching states of the FCMI, four commutation processes for all the main switches are required to achieve the soft-switching conditions in one cycle. For simplification, two switching transitions for S_1 and S_4 are examined below.

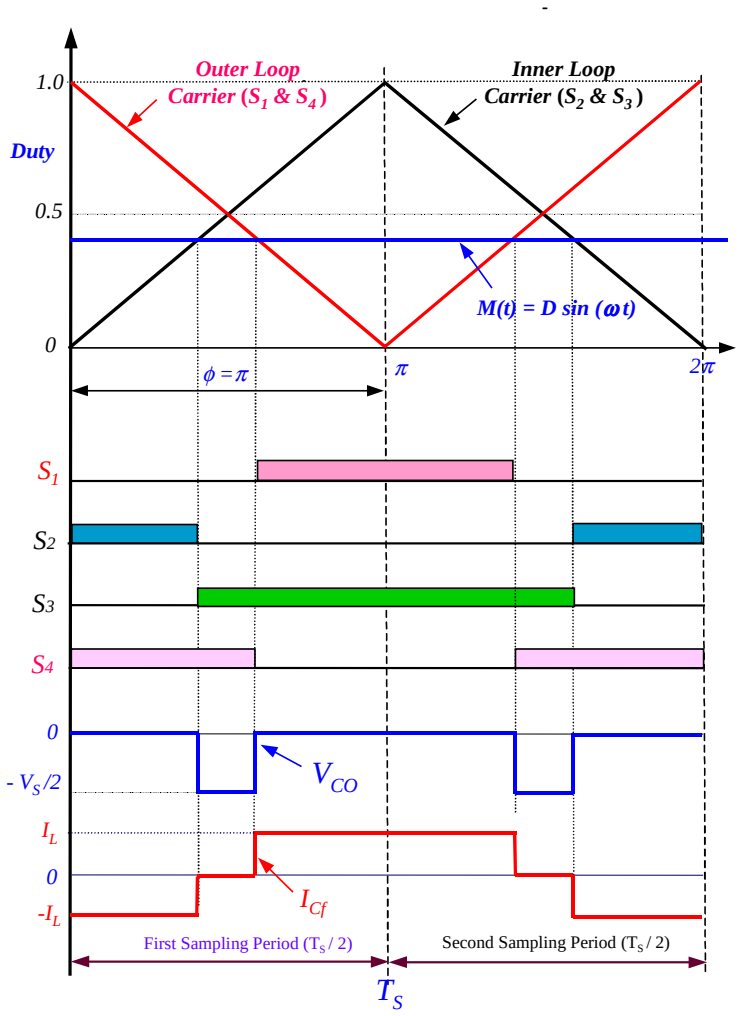

Fig. 2.6. Switching sequences and theirs corresponding voltage and current waveforms of the multilevel inverter.

The theoretical waveforms of two commutation processes and their operational circuits for S_1 and S_4 are illustrated as shown in Fig. 2.7, considering the commutation sequence changes from D_4 to S_1 and from S_1 to D_4. Fig. 2.8 shows the operational circuits of the proposed soft-switching inverter during the commutation process of S_1 and S_4. To explain their operational modes in the intervals (t_0, t_{12}), the twelve different modes are analyzed as follows:

Mode 0 [t_0 - t_1]

Assume that the load current is positive. The two diodes, D_3 and D_4 which are, in the bottom side are conducting the load current of I_L. At this interval, the main switches S_1 and S_2 are turned off and their snubber capacitor voltages are charged at $V_S/2$, respectively.

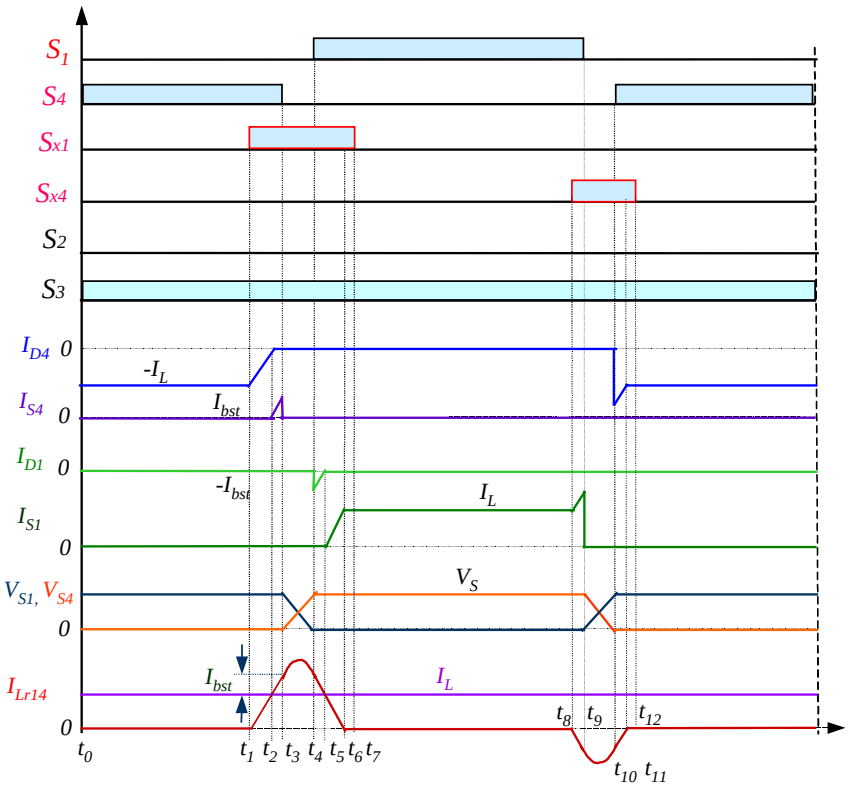

Fig. 2.7. Corresponding voltage and current waveforms during commutations for S_1 and S_4.

Mode 1 [$t_1 - t_2$]

After the auxiliary switch S_{x1} turns on, the inductor current I_{Lr14} (= I_{lk14}) increases linearly until it reaches the load current I_L. At this time, the current in D_4 starts to decrease slowly to zero. The slope can be determined as a function of the resonant inductor and dc source as below.

$$\frac{di_{Lr14}}{dt} = \frac{V_S - V_{cf2}}{L_{lk14}} = \frac{V_S / 2}{L_{lk14}} \tag{2-1}$$

At t = t_2, the charging current of the resonant inductor I_{Lr14} is equal to I_L. The I_{D4} reaches zero. The charging time can be calculated by the below expression:

$$t_2 - t_1 = \frac{L_{lk14} \cdot I_L}{V_S / 2} \tag{2-2}$$

Mode 2 [$t_2 - t_3$]

When the inductor current I_{Lr14} exceeds the load current I_L, the diode current I_{D4} is turned off naturally. During this interval, the main switch S_4 is turned on. This boost current can be expressed as:

$$i_{bst} = \frac{V_S / 2}{L_{lk14}} \cdot (t_3 - t_2) \tag{2-3}$$

This boost current helps to quickly discharge the capacitor voltage across the main switch of S_1.

Mode 3 [$t_3 - t_4$]

After S_4 turns off, the resonant inductor and capacitor start to resonate to discharge the capacitor voltage of S_1. The voltage across the resonant capacitor of S_1 reaches zero and V_{S4} increases to $V_S/2$. Thus, the resonant capacitor C_{r1} (= C_{S1}) and resonant inductor L_{Lr14} (= L_{lk14}) establish a resonant path. At this interval t (= $t_4 - t_3$), the initial conditions are defined as $V_{S1}(0) = V_S/2$, V_{S4}

(0) = 0, and i_{Lr14} (0) = I_L. Under these conditions, the resonant capacitor voltage and inductor current can be expressed as:

$$v_{Cr_1}(t) = V_S \cdot (1 - cos(\omega_{r14} t)) / 2$$

$$i_{Lr14}(t) = I_L + i_{bst} + \frac{V_S / 2}{Z_{Lr14}} \cdot sin(\omega_{r14} t) \quad (2\text{-}4)$$

where,

$$\omega_{r14} = \frac{1}{\sqrt{L_{Lr14} \cdot C_r}} \ (\because C_r = C_{r4})$$

$$Z_{Lr14} = \sqrt{L_{Lr14} / C_r} \quad (2\text{-}5)$$

The resonant period ends when V_{Cr1} reaches zero at t = t_4. The parallel diode of S_1 provides a current path for the resonant current.

Mode 4 [$t_4 - t_5$]

After the resonant period, the stored inductor current slowly starts to decrease through the resonant tank. During this interval, negative voltage is applied to the resonant inductor by the usage of a coupled inductor. Therefore the slope of the resonant inductor decreases linearly, and this interval ($t_4 - t_5$) follows as:

$$t_5 - t_4 = \frac{L_{r14} \cdot I_L}{V_S / 2} \quad (2\text{-}6)$$

Mode 5 [$t_5 - t_6$]

At t = t_5, the resonant current becomes equivalent to the load current, and when I_{Lr14} is less than I_L, the switch current I_{S1} is turned on under at zero-voltage condition. When the resonant current falls below I_L, the commutation will naturally occur from D_4 to S_1 under zero-voltage condition.

Mode 6 [$t_6 - t_7$]

After t = t_6, the diode D_{x1} will be turned off at zero-current condition and the main switch S_1 quickly reaches I_L. Conducting the D_{x1} stabilizes the circulating path of the magnetizing current through the coupled inductor during this mode period. After the elimination of the magnetizing current, the auxiliary switch S_{x1} is turned off at zero current condition.

Mode 7 [$t_7 - t_8$]

After t_7, all of the commutations process completely when the auxiliary switch S_{x1} is turned off at zero-current condition. The operation of the inverter is in such a steady state that S_1 and S_3 are conducting the load current of I_L through the floating capacitors C_{f1}. At this period, the flying capacitor C_{f1} charges at $V_S/2$.

Mode 8 [$t_8 - t_9$]

In order to achieve the soft-switching for S_4, the auxiliary switch S_{x4} turns on. Then, the inductor current I_{Lr14} increases linearly until it reaches the load current I_L similar to **Mode 1**. Thus, the current of I_{S1} starts to increase slowly until t_9. The current can be determined as a function of the boosting current and resonant inductor as below.

$$i_{S1} = I_L + \frac{V_S / 2}{L_{lk14}} \cdot (t_9 - t_8) \qquad (2\text{-}7)$$

On the other hand, the current of the resonant inductor I_{Lr14} starts to charge during this period. The charging time can be determined by the control scheme because the opposite switches do not need much high resonant current to achieve zero-voltage conditions. Thus, the charging time can be minimized depending on the load condition. This boost current helps to quickly discharge the capacitor voltage across the main switch of S_4.

Mode 9 [$t_9 - t_{10}$]

As soon as S_1 turns off, the resonant inductor and capacitor start to resonate in order to discharge

the capacitor voltage of S_4. The voltage across the resonant capacitor of S_4 reaches zero and V_{S1} increases to $V_S/2$. Thus, the resonant capacitor C_{r4} (= C_{S4}) and resonant inductor L_{Lr14} (= L_{lk14}) establish a resonant path. At this interval t (= $t_{10} - t_9$), the initial conditions are defined as $V_{S4}(0) = V_S/2$, $V_{S1}(0) = 0$, and $i_{Lr14}(0) = I_L$. Under these conditions, the resonant capacitor voltage and inductor current can be expressed as:

$$v_{Cr_4}(t) = V_S \cdot (1 - cos(\omega_{r14} t)) / 2$$

$$i_{Lr14}(t) = i_{bst} + \frac{V_S / 2}{Z_{Lr14}} \cdot sin(\omega_{r14} t) \qquad (2\text{-}8)$$

The resonant period ends when V_{Cr4} fully reaches zero at $t = t_{10}$. The parallel diode of S_4 provides a current path for the resonant current.

Mode 10 [$t_{10} - t_{11}$]

After the resonant period, the stored inductor current slowly starts to discharge through the resonant tank. During this interval, negative voltage is applied to the resonant inductor by using a coupled inductor. Therefore, the slope of the resonant inductor decreases linearly and this interval ($t_{10} - t_{11}$) follows as:

$$t_{11} - t_{10} = -\frac{L_{r14} \cdot I_L}{V_S / 2} \qquad (2\text{-}9)$$

Mode 11 [$t_{11} - t_{12}$]

At $t = t_{11}$, the resonant current reaches zero and the diode D_{x4} turns off at a zero-current condition. Conducting the D_{x4} stabilizes the circulating path of the magnetizing current through the coupled inductor during this mode period. After the elimination of the magnetizing current, the auxiliary switch S_{x4} is turned off at zero current condition.

Mode 12 [$t_{12} - t_0$]

After t_{12}, all the commutation processes completely end when the auxiliary switch S_{x4} turns off at a zero-current condition. The operation of the inverter is in a steady state such that S_3 and S_4 are conducting the load current of I_L through D_3 and D_4 during a freewheeling current period.

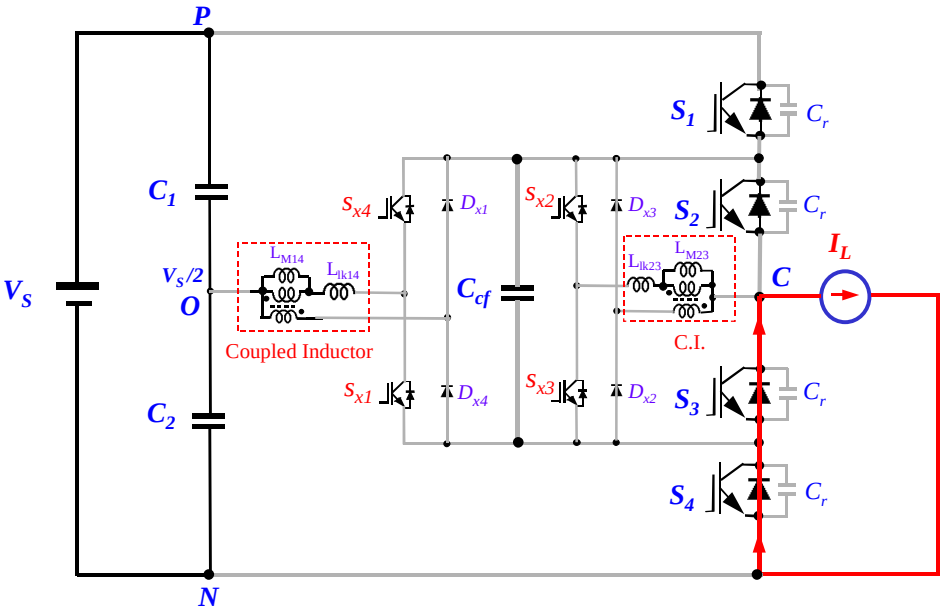

(a) Mode 0 [$t_0 - t_1$]

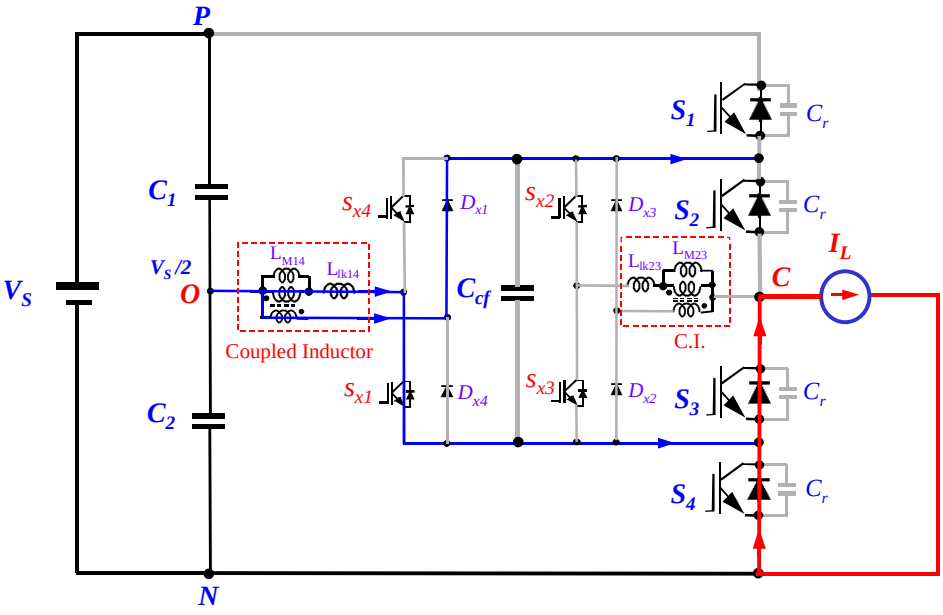

(b) Mode 1 [$t_1 - t_2$]

Fig. 2.8. Operational modes of the commutation sequence.

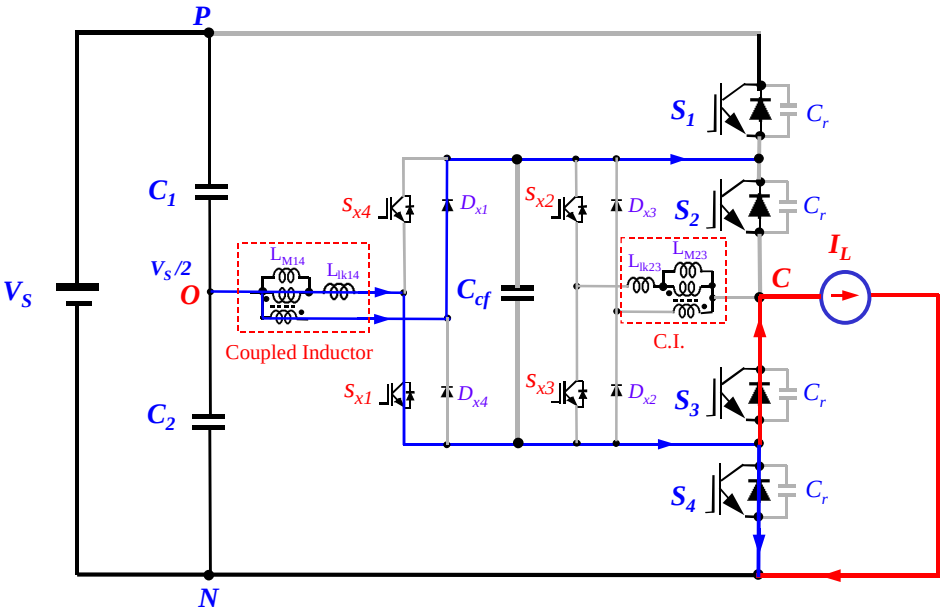

(c) Mode 2 [$t_2 - t_3$]

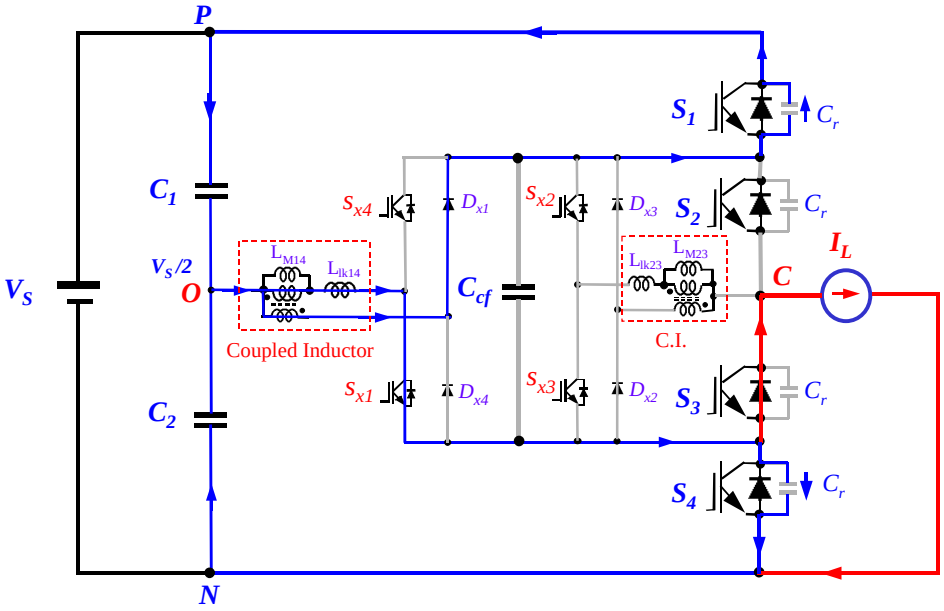

(d) Mode 3 [$t_3 - t_4$]

Fig. 2.8. Operational modes of the commutation sequence (continued).

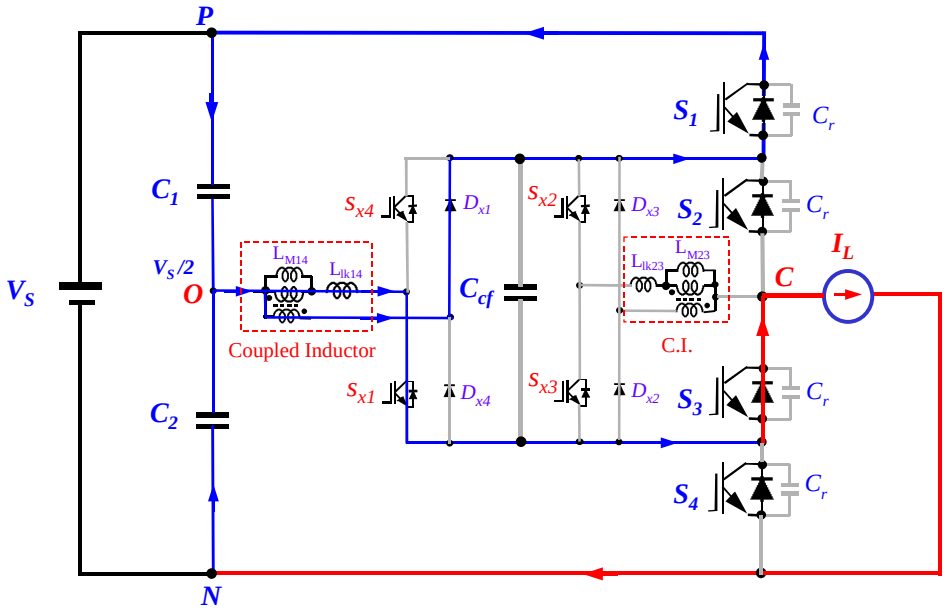

(d) Mode 4 [$t_4 - t_5$]

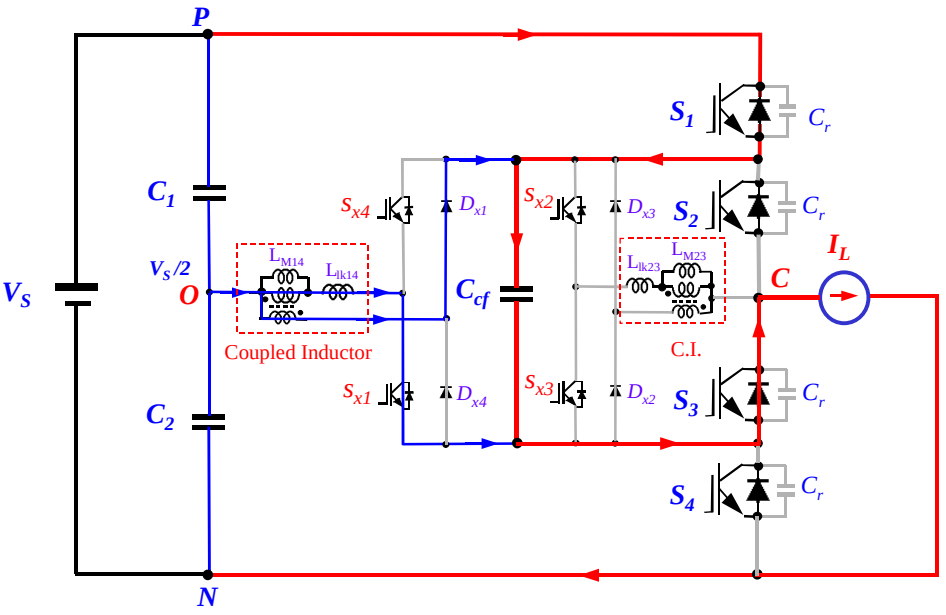

(f) Mode 5 [$t_5 - t_6$]

Fig. 2.8. Operational modes of the commutation sequence (continued).

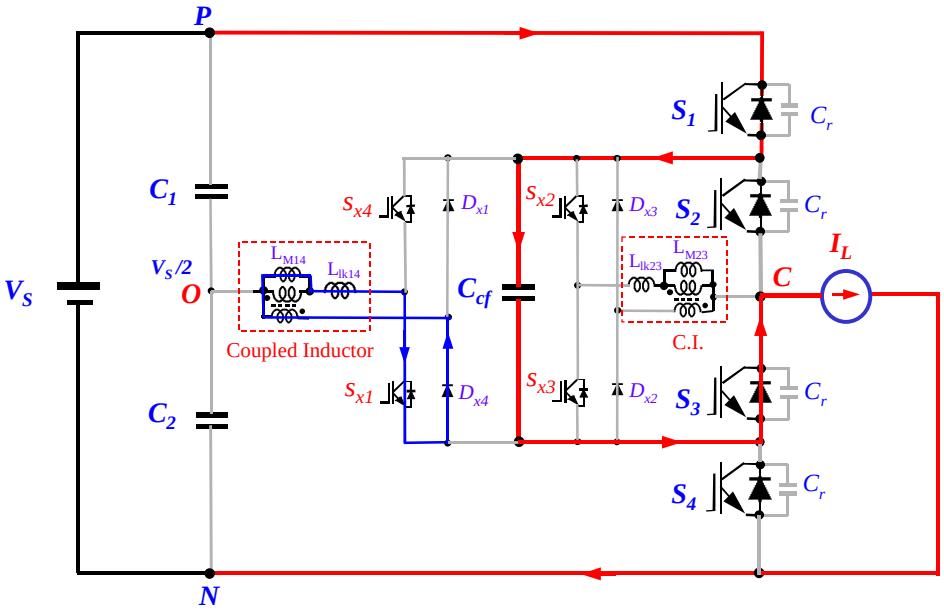

(g) Mode 6 [$t_6 - t_7$]

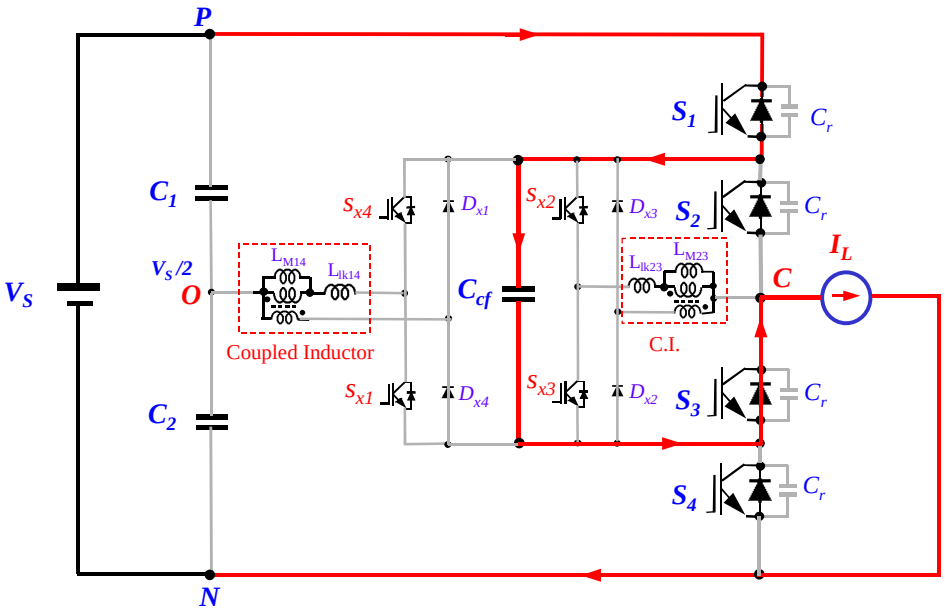

(h) Mode 7 [$t_7 - t_8$]

Fig. 2.8. Operational modes of the commutation sequence (continued).

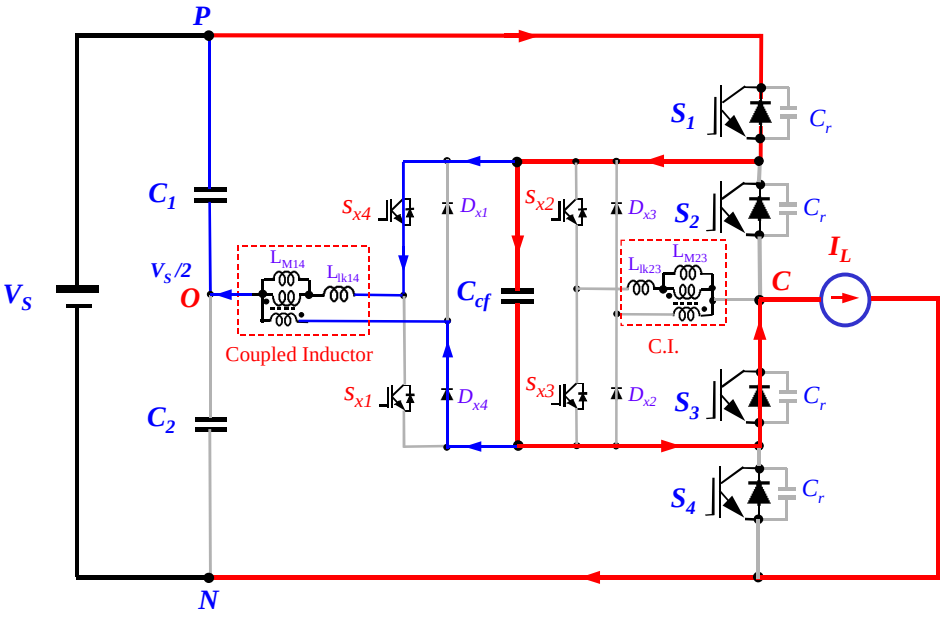

(i) Mode 8 [$t_8 - t_9$]

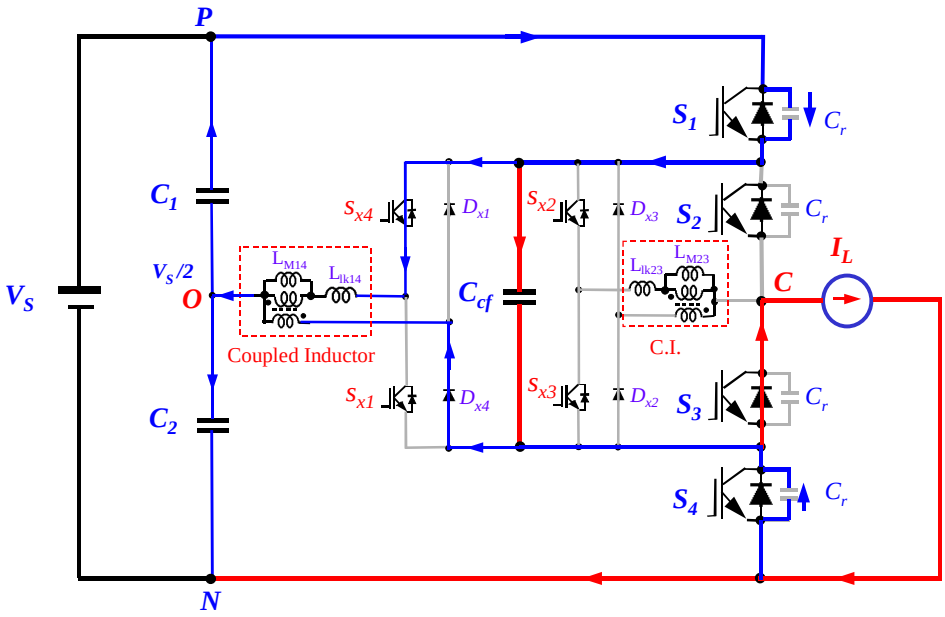

(j) Mode 9 [$t_9 - t_{10}$]

Fig. 2.8. Operational modes of the commutation sequence (continued).

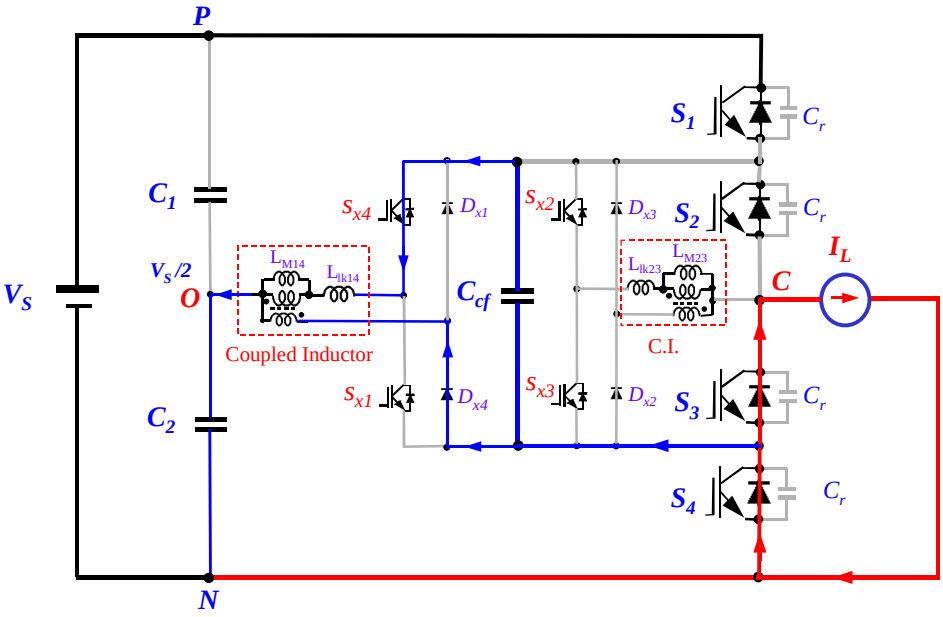

(k) Mode 10 [$t_{10} - t_{11}$]

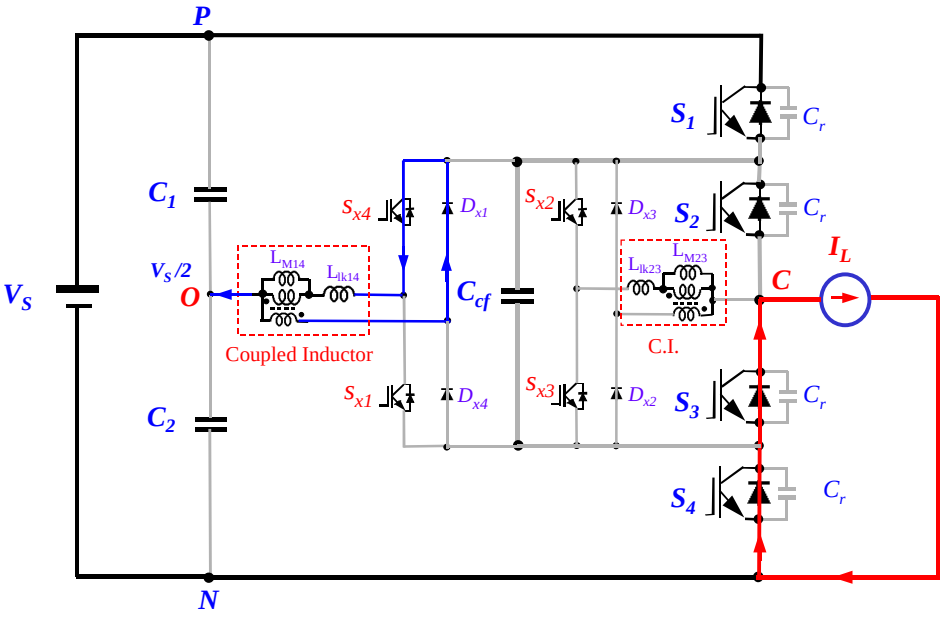

(l) Mode 11 [$t_{11} - t_{12}$]

Fig. 2.8. Operational modes of the commutation sequence (continued).

2.4 CHARACTERISTICS OF SOFT-SWITCHING CIRCUITRY

2.4.1 Coupled Inductor Characteristics

Use of a coupled inductor in the proposed inverter provides attractive features, including the following.

1) The peak current rating of the auxiliary switch can be reduced to a little over half of the resonant inductor current needed to enable the ZVT operation.
2) The charge stored in the resonant tank components can easily removed.

Therefore, the use of the coupled inductor helps achieve a reduction of the magnetic size and weight in the inverter. It enables one to get a higher performance inverter. However, a major limitation of the use of coupled inductors is that they require a magnetically coupled structure. This results in a difficult inductor design with a reset mechanism. Even a coupled inductor mechanism allows more versatility in designing the soft-switching circuit. In addition, since a residual leakage current caused by a small mutual inductance of the coupled inductor fully charges and discharges depending on the switching duties, a reset mechanism is required for the proposed inverter while the auxiliary switch turns off.

2.4.2 Reset Mechanism with Saturable Inductor

For a successful soft-switching operation for inner loop IGBTs, it is necessary to block a circulating current through the coupled inductor. The circulating current is always found whenever coupled inductors are used in the ZVT inverters. This is because the inductor has no blocking capability during the freewheeling mode. In order to eliminate or reduce the circulating current through the coupled inductor, a saturable inductor that has an initially large inductance before its saturation can be used if necessary. Using the saturable inductor helps not only to block the circulating current during steady state but also to reset the magnetizing current flowing through the coupled inductor while the auxiliary switch turns off.

Fig. 2.9 shows the reset mechanism of the coupled inductor when using a saturable inductor. This figure explains that the saturable inductor provides a reset path for the magnetizing current by blocking it. At this time, the voltage across the saturable inductor is shared to a half of the flying capacitor voltage so that the voltage-second of the coupled inductor can be reduced. This results in better performance when completing soft-switching operations.

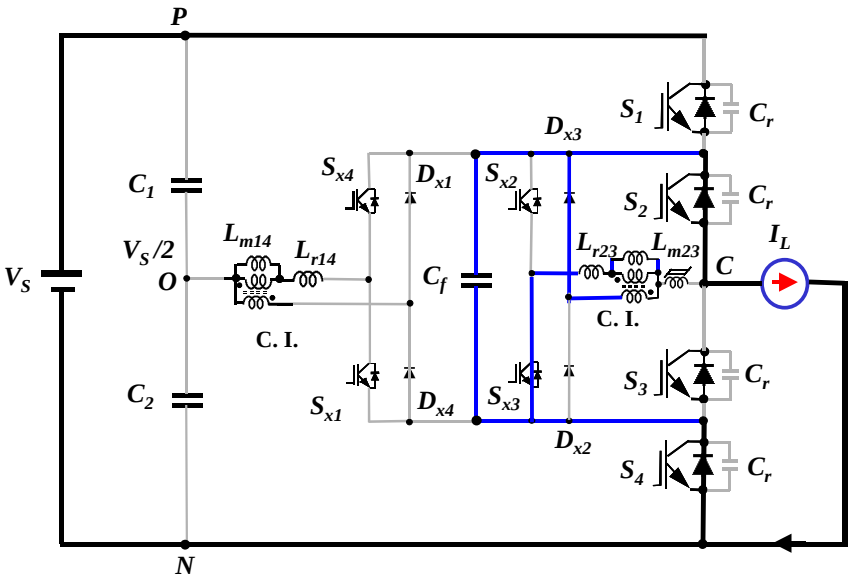

(a) Reset mode

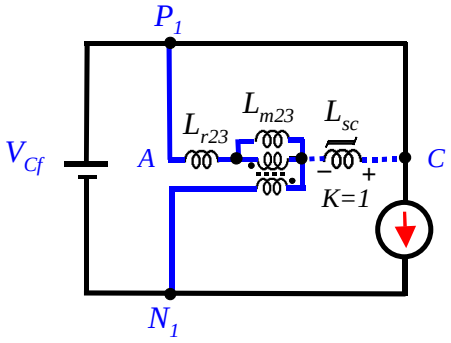

(b) Blocking function

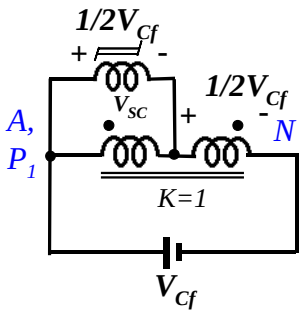

(c) Voltage sharing

Fig. 2.9. Reset mechanism of the coupled inductor with a saturable inductor.

2.4.3 Soft-switching Control

When designing the control circuit and its time sequence, control flexibility with adjustable timing is required for the wide operation ranges. To stabilize the operation corresponding to the PWM signal as an input signal, a monostable multivibrator device is preferred. Besides, the protection circuit for elimination of the short pulse is also added to ensure zero voltage operation under any load condition. For timing control criteria, the relationship between deadtime of the main device and the discharging time of the stored energy of the resonant capacitor should be related to the control of the resonant circuit. There are two possible solutions to implement the proposed inverter: fixed timing control and variable timing control.

Fig. 2.10 shows the control block diagram of the proposed inverter and its gate signals for soft-switching operations. The gate signals of S_1-S_4 for the phase A-leg circuit have a time delay of T_D, and the auxiliary switch signals of $S_{x1} - S_{x4}$ have a fixed short pulse of T_{aux} generated by the rising edge of the sinusoidal pulse-width-modulation (SPWM) signals. A SPWM method can be adopted for the load current regulation.

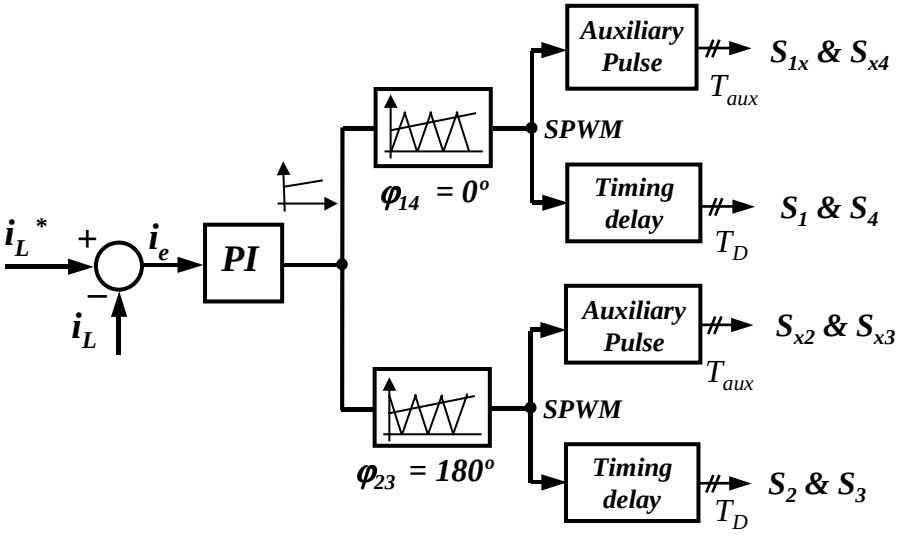

(a) Soft-switching control scheme

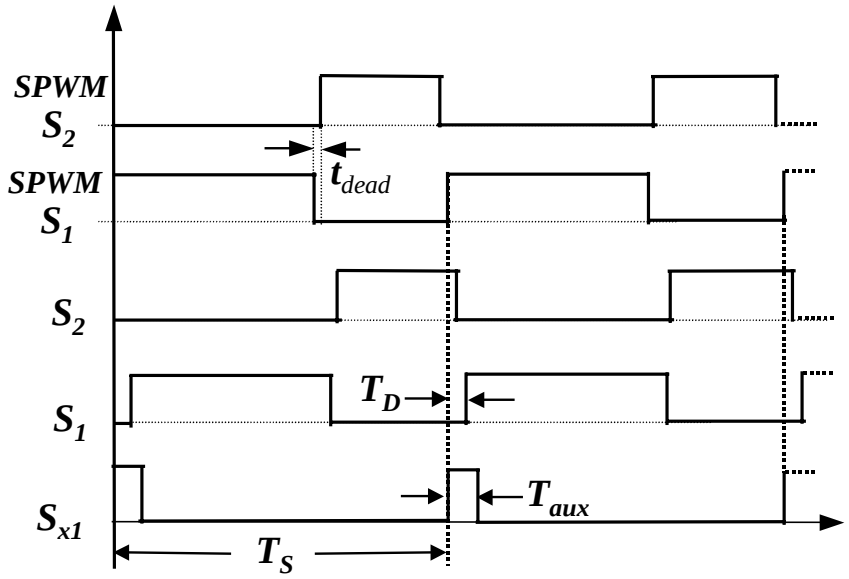

(b) Gate signals

Fig. 2.10. Control block diagram for soft-switching control.

2.5 SIMULATION AND EXPERIMENTAL RESULTS

In order to validate the proposed inverter, computer simulations and experiments were conducted. In simulation, computer-aided analysis software such as the Pspice program is used. This is basically to further study the auxiliary resonant components and conducting timing selections. The resonant circuit parameters are selected as L_r = 3μH, C_r = 0.14μF, and T_{aux} = 5μs.

Fig. 2.11 shows the operational waveforms of the single-phase three-level FCMI under hard-switching operations. As expected, the three-level output voltage waveform was observed by setting control signals under the conditions of the equal duty cycle and π phase shift.

Fig. 2.12 shows the simulated voltage and current waveforms of the soft-switching inverter with a fixed time of 5μs. The results indicate that the proposed inverter achieves the zero-voltage condition under turn-on.

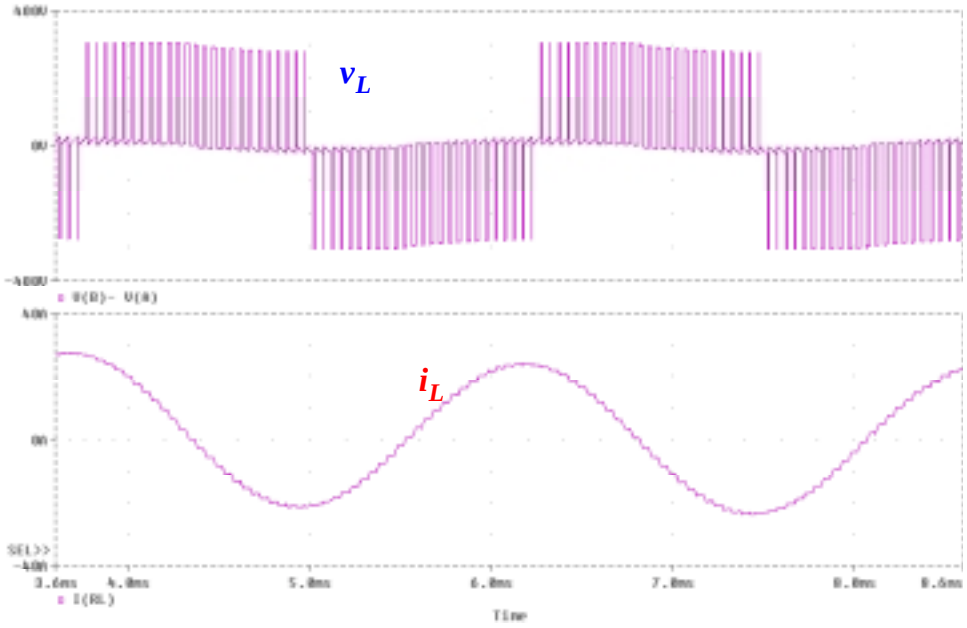

Fig. 2.11. Simulated output voltage and current waveforms of a single-phase three-level inverter with flying capacitors.

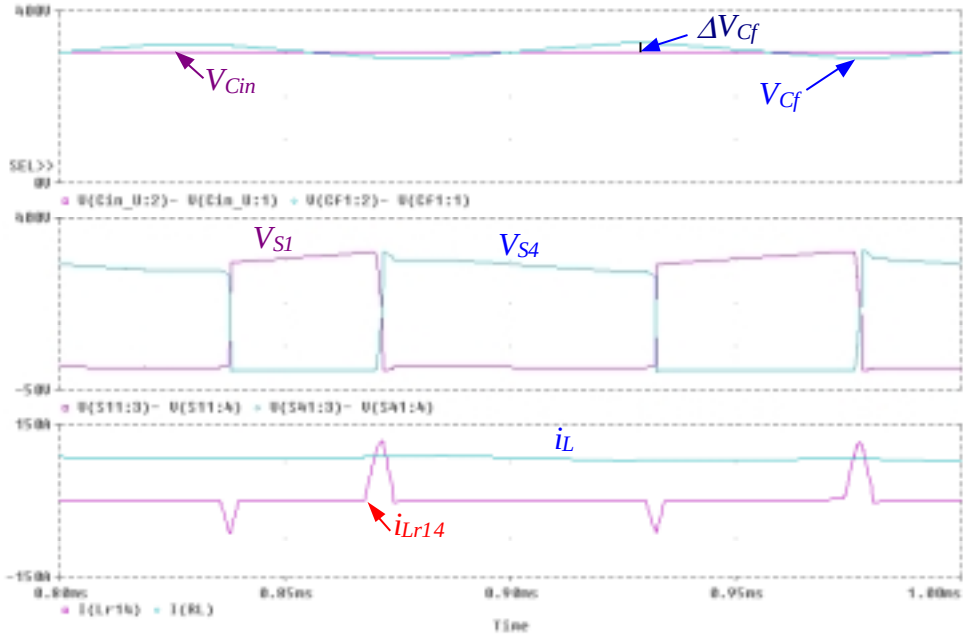

Fig. 2.12. Simulated voltage and current waveforms of the soft-switching inverter with fixed time of $T_{D.}$

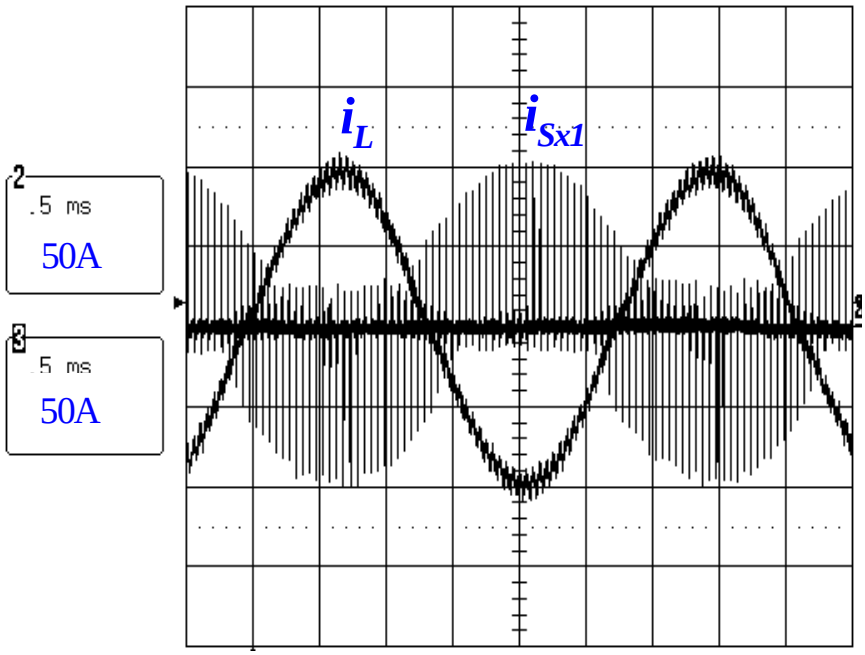

Fig. 2.13. Experimental current waveforms of the inverter under soft-switching operations.

Fig. 2.13 shows the experimental current waveforms of the inverter with variable time. The variable timing control corresponding to load current variations is used on the auxiliary switch circuitry. This results in a reduction of the conduction loss.

Fig. 2.14 shows the key waveforms of the proposed inverter with inductor coupling. Results from Fig. 2.14(a) indicate that the inverter achieved a zero-current turn-off to the auxiliary switches during commutation processes. As expected, the peak resonant current of the coupled inductor winding, I_{Sx1}, was obtained at a little over half of the resonant inductor current. The resonant current, I_{Lr14}, which needs to achieve a ZVT condition to S_1, was required to be larger than that of the load current. The magnitude and duration of the resonant current through the coupled inductor depends on the load current directions. Fig. 2.14(b) shows the voltage and current waveforms across the coupled inductor and saturable inductor under soft-switching commutations. As a result, the use of a saturable inductor in the soft-switching circuit can nearly block the reset current at the end of the commutation process.

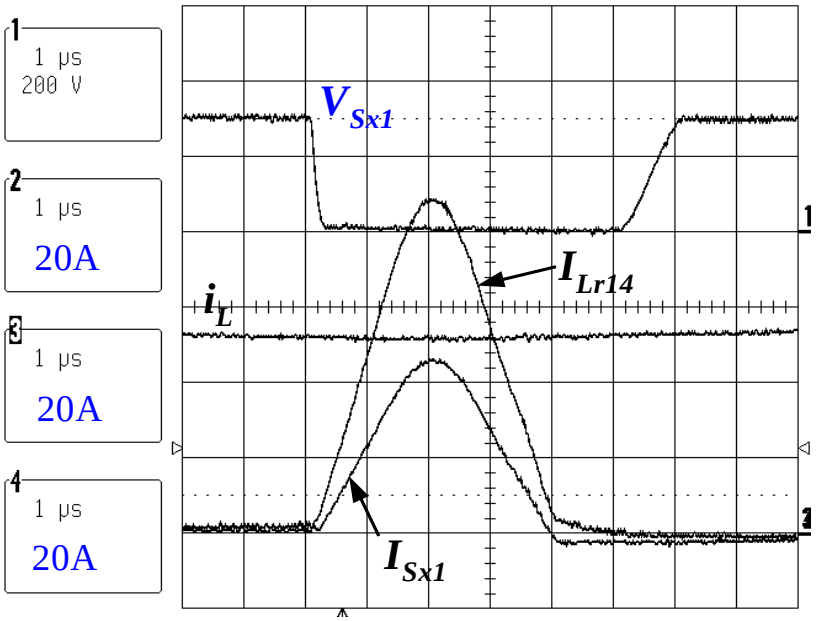

(a) Auxiliary switch and resonant inductor

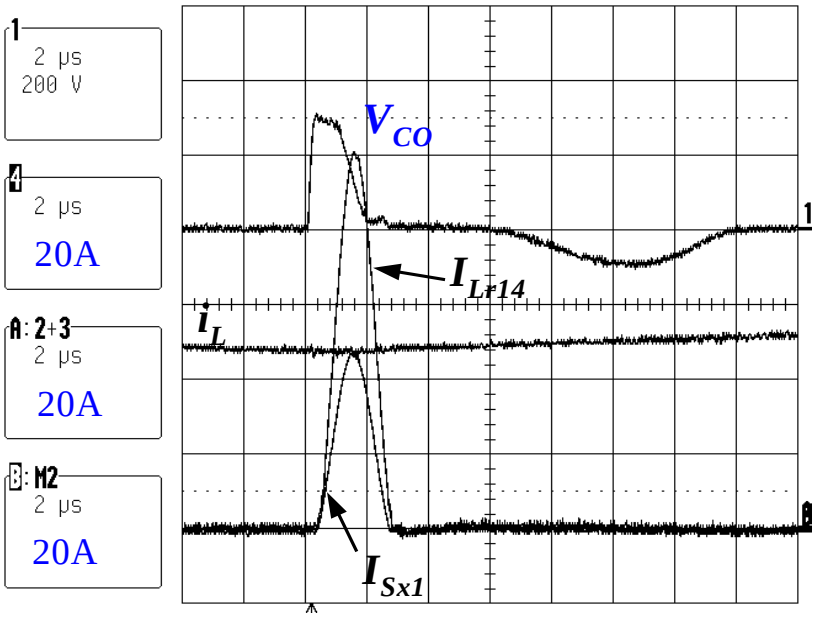

(b) Resonant branch

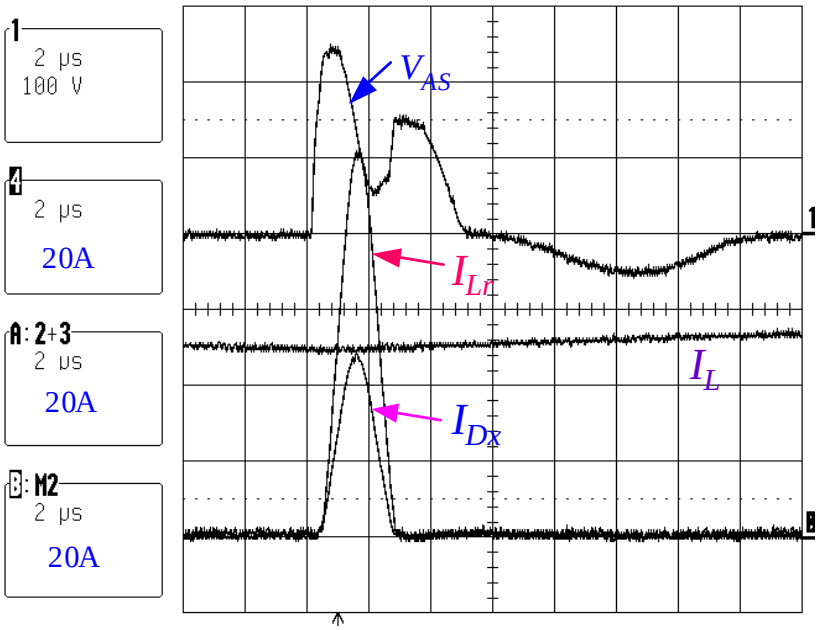

(c) Coupled inductor and its blocking voltage

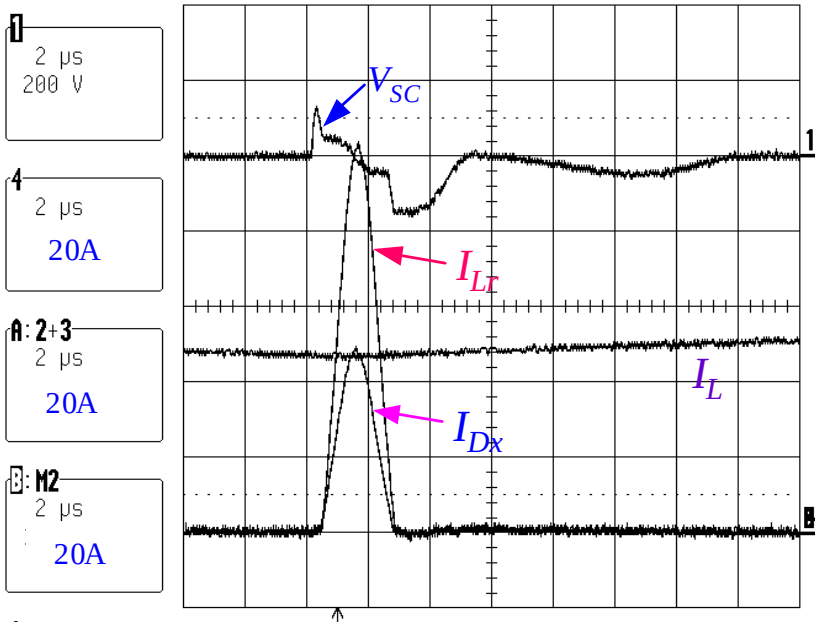

(d) Saturable inductor and its blocking voltage

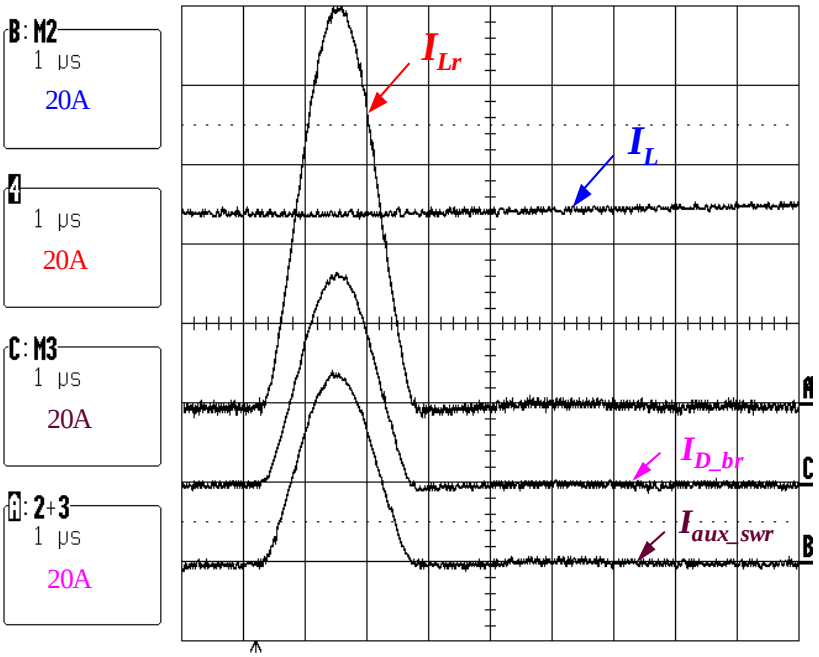

(e) Current sharing between coupled windings

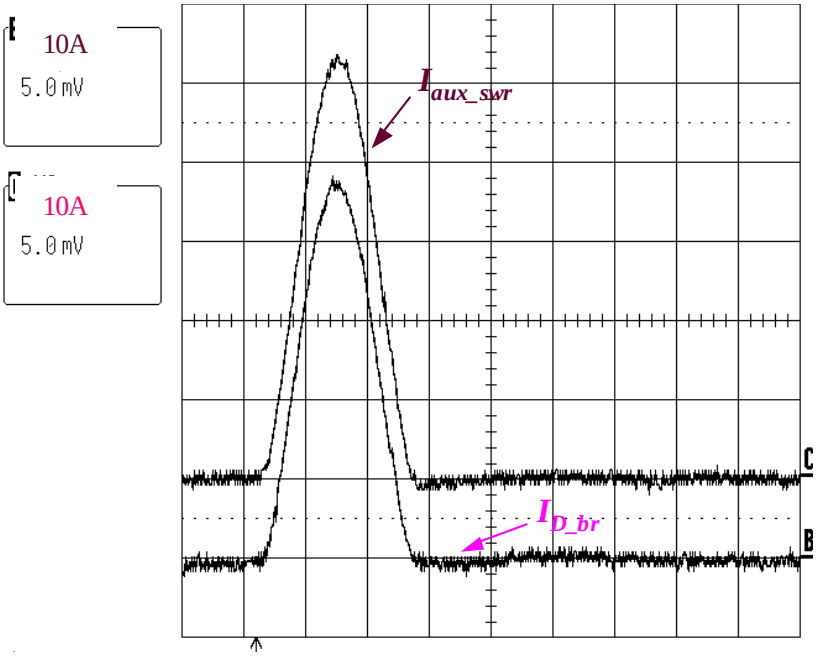

(f) Auxiliary switch and diode currents

Fig. 2.14. Experimental voltage and current waveforms of S_{x1} under soft-switching operations.

2.6 CONCLUSION

In this chapter a new soft-switching flying capacitor multilevel inverter has been introduced and verified through both simulation and experimentation. The proposed inverter used a ZVT soft-switching circuitry with inductor coupling, in which the auxiliary devices have less voltage and current ratings. Thus, the proposed inverter has the advantages of lower voltage and current ratings for auxiliary switches and diodes, achieved by using a coupled inductor and midpoint rail between the DC capacitors.

Results indicated that the proposed inverter achieved zero-voltage condition in all of the main switches and zero-current turn-off of the auxiliary switches during the commutation processes.

In this chapter, the development of the proposed soft-switching inverter for active power applications was discussed. The details will be discussed in the next chapter.